



Article

# MLLT11 Regulates Endometrial Stroma Cell Adhesion, Proliferation and Survival in Ectopic Lesions of Women with Advanced Endometriosis

Katharina Proestling <sup>1</sup>, Heinrich Husslein <sup>1</sup> , Quanah James Hudson <sup>1</sup> , Matthias Witzmann-Stern <sup>1</sup>, Barbara Widmar <sup>1</sup>, Zsuzsanna Bagó-Horváth <sup>2</sup>, Lejla Sandrieser <sup>1</sup>, Alexandra Perricos <sup>1</sup> , René Wenzl <sup>1</sup> and Iveta Yotova <sup>1,\*</sup>

<sup>1</sup> Department of Obstetrics and Gynecology, Medical University of Vienna, Waehringer Guertel 18-20, A-1090 Vienna, Austria; katharina.proestling@meduniwien.ac.at (K.P.); heinrich.husslein@meduniwien.ac.at (H.H.); quanah.hudson@meduniwien.ac.at (Q.J.H.); matthias.witzmann-stern@meduniwien.ac.at (M.W.-S.); barbara.widmar@meduniwien.ac.at (B.W.); lejla.sandrieser@meduniwien.ac.at (L.S.); alexandra.perricos@meduniwien.ac.at (A.P.); rene.wenzl@meduniwien.ac.at (R.W.)

<sup>2</sup> Department of Pathology, Medical University of Vienna, Waehringer Guertel 18-20, A-1090 Vienna, Austria; zsuzsanna.horvath@meduniwien.ac.at

\* Correspondence: iveta.yotova@meduniwien.ac.at; Tel.: +43-1-40400-78280

**Abstract:** *MLLT11* is a gene implicated in cell differentiation and the development and progression of human cancers, but whose role in the pathogenesis of endometriosis is still unknown. Using quantitative RT-PCR and immunohistochemistry, we analyzed 37 women with and 33 women without endometriosis for differences in *MLLT11* expression. We found that *MLLT11* is reduced in the ectopic stroma cells of women with advanced stage endometriosis compared to women without endometriosis. *MLLT11* knockdown in control stroma cells resulted in the downregulation of their proliferation accompanied by G1 cell arrest and an increase in the expression of p21 and p27. Furthermore, the knockdown of *MLLT11* was associated with increased apoptosis resistance to camptothecin associated with changes in BCL2/BAX signaling. Finally, *MLLT11* siRNA knockdown in the control primary stroma cells led to an increase in cell adhesion associated with the transcriptional activation of ACTA2 and TGFB2. We found that the cellular phenotype of *MLLT11* knockdown cells resembled the phenotype of the primary endometriosis stroma cells of the lesion, where the levels of *MLLT11* are significantly reduced compared to the eutopic stroma cells of women without the disease. Overall, our results indicate that *MLLT11* may be a new clinically relevant player in the pathogenesis of endometriosis.

**Keywords:** *MLLT11*; endometriosis; primary endometrial stroma cells; proliferation; cell cycle; adhesion; apoptosis resistance; apoptosis



**Citation:** Proestling, K.; Husslein, H.; Hudson, Q.J.; Witzmann-Stern, M.; Widmar, B.; Bagó-Horváth, Z.; Sandrieser, L.; Perricos, A.; Wenzl, R.; Yotova, I. *MLLT11* Regulates Endometrial Stroma Cell Adhesion, Proliferation and Survival in Ectopic Lesions of Women with Advanced Endometriosis. *Int. J. Mol. Sci.* **2024**, *25*, 439. <https://doi.org/10.3390/ijms25010439>

Academic Editor: David B. Alexander

Received: 21 November 2023

Revised: 26 December 2023

Accepted: 27 December 2023

Published: 28 December 2023



**Copyright:** © 2023 by the authors. Licensee MDPI, Basel, Switzerland. This article is an open access article distributed under the terms and conditions of the Creative Commons Attribution (CC BY) license (<https://creativecommons.org/licenses/by/4.0/>).

## 1. Introduction

Endometriosis is an estrogen-driven gynecological condition affecting up to 10% of the women of a reproductive age [1]. It is characterized by the formation of endometriosis lesions outside the uterus, predominantly in the peritoneal cavity. These ectopic growths contain endometrial glands and stromal cells resembling endometrium [2]. It is a chronic inflammatory disease, commonly resulting in symptoms including chronic pelvic pain, dysmenorrhea, dyspareunia and fatigue and is often associated with infertility, strongly affecting the quality of life of affected women [2]. Currently, peritoneal endometriotic lesions are mainly diagnosed using laparoscopy, as no clinically approved diagnostic biomarkers exist. The nonspecific nature of the symptoms and the lack of reliable diagnostic markers, together with uncertain disease etiology, often leads to a significant delay in the diagnosis and treatment of patients with the disease [3]. Although the etiology of the

disease remains unclear, the retrograde transport of menstrual endometrial debris into the peritoneal cavity is the most widely accepted hypothesis for the origin of ectopic lesions [4]. Endometriosis is a benign disease, which shows progressive and invasive growth, a high recurrence rate and tends to spread [5,6]. In order for endometriotic lesions to develop, endometrial cells in the peritoneal cavity must adhere, proliferate, invade and differentiate while avoiding or coopting the immune system [7,8]. However, the growth of endometriotic lesions is tightly controlled, while the uncontrolled proliferation of ectopic lesions is rarely observed in endometriosis [9].

Nevertheless, a range of studies have shown that genes with an altered expression in a diversity of cancers are also deregulated in endometriotic tissue [10] and may contribute to the pathogenesis of endometriosis. For example, patients with endometriosis have a higher risk of developing some types of ovarian cancer [11]. Previous reports have shown that shared alterations in the expression levels of certain genes in both endometriotic lesions and endometriosis-associated ovarian carcinomas exist [12]. This indicates that examining deregulated genes in both diseases may help understand the pathogenesis of endometriosis and to define the molecular basis for the differences between these benign and malignant conditions.

Mixed-lineage leukemia translocated to 11 (*MLLT11*), also called the ALL1-fused gene from the chromosome 1q (*AF1Q*) gene, has been found to be overexpressed in ovarian cancer and to be associated with a poor patient outcome [13]. The gene encodes a small 9 kDa protein originally defined as an oncogenic factor associated with a genetic translocation (t (1;11) (q21;q23)) present in certain types of leukemia [14,15]. The gene functions as an oncogene by regulating the epithelial to mesenchymal transition of ovarian cells to ensure their high plasticity, increased invasiveness and motility [13]. In ovarian cancer cells, the overexpression of *MLLT11* was also associated with an activation of WNT/beta-catenin/S100A4 oncogenic signals, resulting in malignant tumor progression and metastasis formation and reduced sensitivity to cancer therapy [13]. On the other hand, *MLLT11* has also been identified as mediator of basal and 4-HPR-induced apoptosis in ovarian cancer cells, illustrating the somewhat contradictory dual proapoptotic and protumorigenic behavior of the gene in ovarian cancer cells [16]. A functional role of *MLLT11* in tumor progression was also reported in human breast [17] and endometrial carcinomas [18], as well as in a number of other human solid tumors [19,20]. In contrast to this oncogenic role, in the nervous system, *MLLT11* functions as a tumor suppressor, with a high level of expression in normal brain tissues compared with decreased expression correlating with the malignant tumor grade [21].

Despite the considerable advances made in understanding the role of *MLLT11* in human carcinogenesis and in cortical projection neuron morphogenesis during development [22], the role of this gene in the pathogenesis of endometriosis remains unclear. Therefore, in this study, we analyzed the differences in the expression levels of *MLLT11* in women with and without endometriosis and evaluated the role of this gene in disease pathogenesis using primary endometrial stroma cells.

## 2. Results

### 2.1. *MLLT11* Is Downregulated in Ectopic Lesions of Women with Stage III and IV Endometriosis

To identify changes that may occur in *MLLT11* expression levels in endometriosis, we compared the control endometrium of women without endometriosis to ectopic lesions using qRT-PCR. This included 23 women without and 31 women with endometriosis—with some patients contributing more than one lesion sample (Supplementary Table S1A). This showed that *MLLT11* expression is downregulated (0.49 median fold change, adjp value = 0.010) in ectopic lesions of women with endometriosis compared to the eutopic endometrium of women without the disease (Figure 1a). Women with severe stage endometriosis (the revised American Fertility Society (rAFS) score III + IV) showed significantly lower levels of *MLLT11* expression compared to women without the disease (0.53 median fold change, adjp value = 0.045, Figure 1b). However, it cannot be excluded

that *MLLT11* expression is also reduced in rAFS I + II stage ectopic tissue, given that a relatively small number of samples of this type of tissue were examined ( $n = 7$ ). *MLLT11* expression did not significantly vary during the menstrual cycle in either the control or ectopic tissue (Figure 1c).

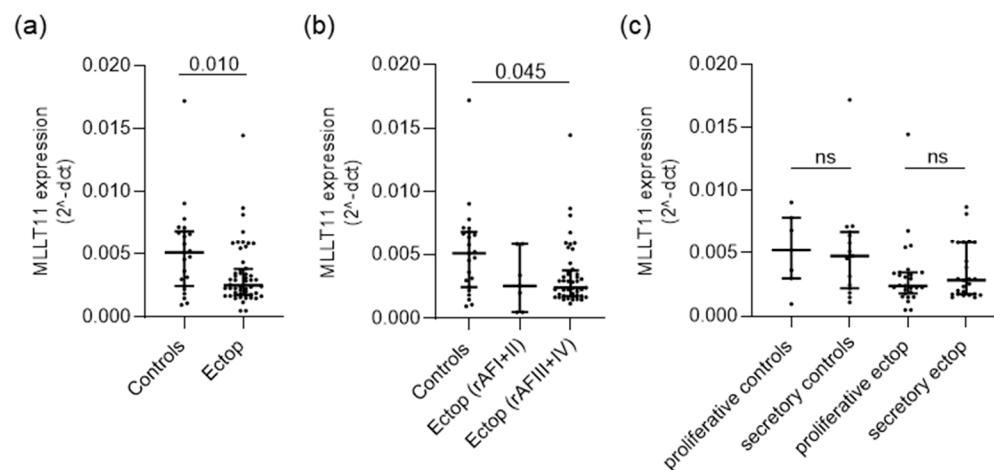


**Figure 1.** *MLLT11* mRNA expression is reduced in endometriosis lesions. (a) Gene expression of *MLLT11* is significantly decreased in ectopic lesions ( $n = 52$ ) compared to the eutopic endometrium of women without endometriosis ( $n = 23$ ). (b) Compared to controls, ectopic *MLLT11* expression does not significantly change in mild disease (rAF I + II,  $n = 7$ ) but shows a significant decrease in more severe endometriosis (rAF III + IV,  $n = 45$ ). Disease stages according to revised American Fertility Society (rAF) scores. (c) *MLLT11* expression does not significantly differ between the proliferative ( $n = 7$ ) and secretory ( $n = 15$ ) stages of the menstrual cycle in control eutopic endometrium or ectopic lesions (proliferative  $n = 27$ , secretory  $n = 25$ ). *MLLT11* gene expression in (a–c) was normalized to ACTB, and data are presented as scatter dot plots including the median relative expression levels and interquartile ranges for each group. Data were analyzed using Mann–Whitney test (a) or Kruskal–Wallis test adjusted for multiple testing using Dunn’s multiple comparisons test (b,c). Adjusted p values ( $\text{adj}p$ )  $< 0.05$  were considered significant, with nonsignificant differences indicated by ns. Controls: endometrial tissue of women without endometriosis, Ectop: tissues from endometriosis lesions.

Next, we used immunohistochemistry to localize *MLLT11* protein expression in the endometrial tissue. As paraffin-embedded tissue was not available for all samples included in the mRNA expression analysis cohort, we had to collect additional samples. Therefore, the sample cohort used for the IHC analysis had only a 40.4% overlap with the sample cohort used for the mRNA expression analysis and, in the end, included 24 women without and 19 women with endometriosis—with some patients contributing more than one lesion sample (Supplementary Figure S1a and Table S1b). In addition, to be able to define the endometrial stroma cell population within the lesions, we stained all ectopic tissue samples with CD10, a verified endometrial stroma marker [23] (Figure 2a).

Our IHC analysis showed that *MLLT11* is expressed in both stromal and epithelial cells but appeared to show differences between these two compartments (Figure 2b). The quantification of staining showed that the levels of *MLLT11* in glandular epithelial cells did not differ between eutopic control endometrium and endometriotic lesions (Figure 2c, left). When we stratified the analysis according to the endometriosis disease stage and menstrual cycle phase, we also did not see differences in the levels of glandular epithelial cell *MLLT11* expression between the groups (Figure 2c, middle and right).

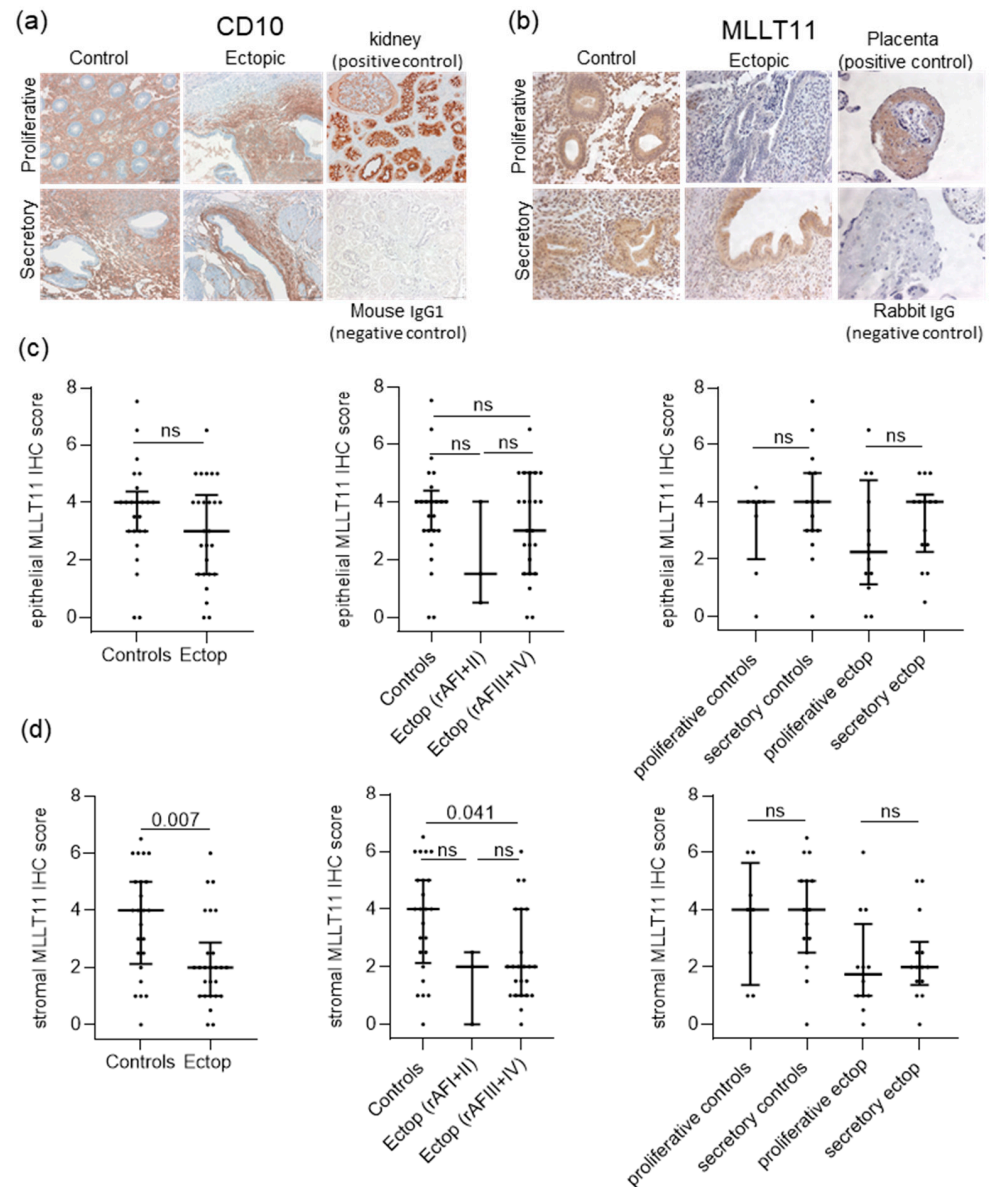


**Figure 2.** Immunohistochemical analyses of MLLT11 expression levels in ectopic endometriosis lesions ( $n = 26$ ) and in control eutopic endometrium from women without endometriosis ( $n = 24$ ). (a) Representative pictures of CD10 staining in tissues of control and ectopic endometrium in the proliferative and secretory menstrual cycle phases are shown at a magnification of  $200\times$ . (b) Representative pictures of MLLT11 staining in controls and ectopic endometrium in the proliferative and secretory menstrual cycle phases. (c,d) The intensity (0–3) and the percentage (0–3) of the stained cells were assessed and combined to define the final IHC score (0–9). For statistical evaluation of the protein MLLT11 score, (c) epithelial and (d) stromal immunostainings were analyzed separately at magnification of  $200\times$ . (c,d, middle) MLLT11 protein expression in mild (rAF I + II,  $n = 3$ ) and more severe (rAF III + IV,  $n = 23$ ) disease stages (revised American Fertility Society (rAF) score). (c,d, right) MLLT11 protein expression does not significantly differ between the proliferative and secretory stages of the menstrual cycle in control endometrium ( $n = 8$  and  $15$ , respectively) or ectopic lesions ( $n = 12$  and  $14$ , respectively). All results (c,d) are expressed as scatter dot plots including the median relative expression levels and interquartile ranges in each group. Data were analyzed using Mann–Whitney tests (c,d left) or Kruskal–Wallis test adjusted for multiple testing using Dunn’s multiple comparisons test (c,d middle and right). Adjusted  $p$  values (adjp)  $< 0.05$  were considered significant. The nonsignificant differences are indicated by ns. Control: endometrial tissue of women without endometriosis, Ectop: tissues from endometriosis lesions.

In contrast, in the stromal cell compartment, *MLLT11* positive cells were significantly reduced in the ectopic lesions (0.5 median fold change, *adjp* value = 0.007) when compared to the eutopic control endometrium (Figure 2d, left). This indicates that the *MLLT11* reduction seen in the ectopic lesions at the RNA level is due to reduced gene expression in the stromal cells (Figure 1a). When patients were classified according to their disease stage, a significant reduction in ectopic stromal cell *MLLT11* expression was only seen in the advanced rAFS III +IV stages of endometriosis (0.5 median fold change, *adjp* value = 0.041) (Figure 2d, middle). However, it cannot be excluded that *MMLT11* expression is also reduced in rAFS I + II stage ectopic stroma, given the small number of samples of this type of tissue (*n* = 3). There was no significant difference in *MLLT11* stromal endometrial expression between the proliferative and secretory phases of the menstrual cycle for any tissue type (Figure 2d, right).

## 2.2. *MLLT11* Knockdown Impairs Cells Proliferation in Primary Endometrial Stromal Cells of Women without Endometriosis

To gain insight into the biological role of reduced *MLLT11* expression in endometriosis lesions, we carried out *MLLT11* siRNA knockdown experiments in primary endometrial stroma cells (hESCs) derived from the endometrial tissue of four patients without endometriosis.

To test if this *in vitro* system accurately represents the situation in patient lesions, we first characterized the purity of our primary cell cultures. All primary cultures derived from either control eutopic endometrium and endometriosis lesions were positive for endometrial stroma cell markers CD10 and vimentin (Figure 3a) and negative for endothelial (*PECAM1*) and epithelial (*EPCAM*) markers (Figure 3b), indicating they represent the endometrial stromal cell compartment.

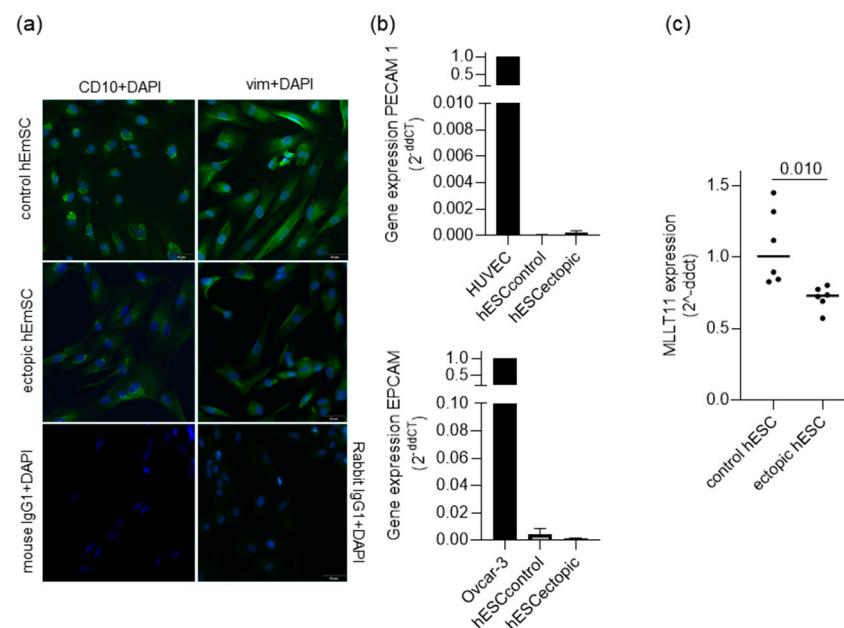


**Figure 3.** Characterization of primary stromal cell cultures. (a) Representative pictures of CD10 (left) and vimentin (right) immunofluorescence staining in primary endometrial stromal cells derived from control eutopic endometrium and ectopic endometriosis lesions. (b) RT-qPCR analysis shows that primary stromal cells derived from control eutopic endometrium (*n* = 4) and ectopic endometriosis lesion (*n* = 4) have very low levels of endothelial and epithelial markers *PECAM1* (top) and *EPCAM* (bottom), indicating their purity. HUVEC and OVCAR-3 were used as positive controls for endothelial and epithelial cells, respectively. Data are presented as bar graphs, and positive controls were set to 1. (c) RT-qPCR analysis of *MLLT11* expression in primary stroma cells derived from control eutopic endometrium (control hESCs, *n* = 6) and ectopic endometriosis lesions (ectopic hESCs, *n* = 6). *MLLT11*

gene expression was significantly lower in ectopic hESCs compared to control hESCs. Data are presented as a scatter blot including the median expression level of each group and analyzed using *t*-test. The patient characteristics of the women from whom the primary cells were derived from are listed in Supplementary Table S1C.

Secondly, we conducted an RT-qPCR analysis of *MLLT11* expression in primary stroma cells derived from six control endometrial samples and six ectopic lesion samples of women with endometriosis (Figure 3c). The results mirrored what was seen in vivo, with a significant reduction in *MLLT11* expression in ectopic compared to control hESCs (0.27 median fold change, *p* value = 0.010) (Figure 3c). Therefore, we proceeded with the *MLLT11* knockdown experiments in four out of six control primary stroma cell lines. We were able to achieve efficient knockdown, with *MLLT11* mRNA reduced to a mean of 5.4% (*p* = 0.009) of the control knockdown cells (Figure 4a). This resulted in a reduction in *MLLT11* protein levels to a mean of 15.7% (*p* = 0.004) of the control knockdown cells (Figure 4b).

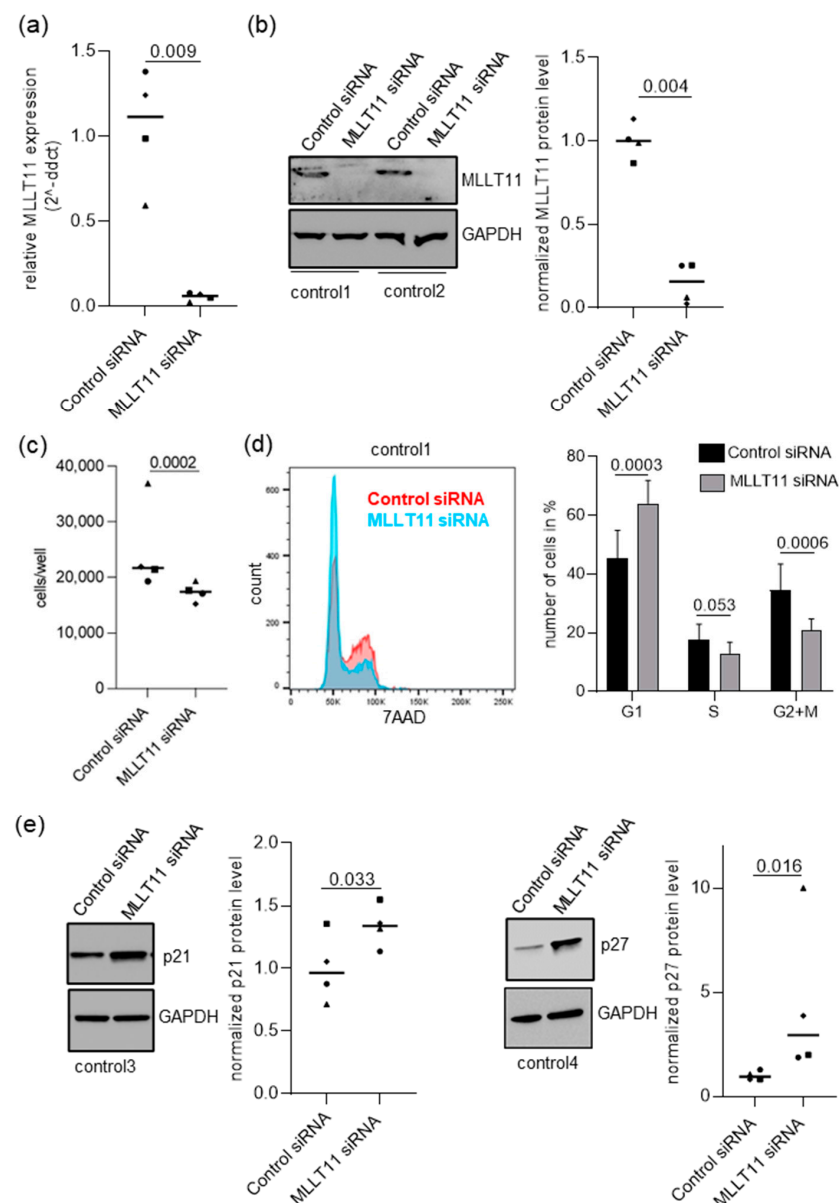


**Figure 4.** *MLLT11* knockdown leads to an increase in cells in the G1 phase and a decrease in cells in the S and M+G2 phases associated with an increase in p21 and p27 levels. (a) *MLLT11* gene and

(b) protein expression after *MLLT11* siRNA knockdown experiments in primary stroma cells obtained from endometrial tissue of four women without the disease. (c) Reduced proliferation rate in *MLLT11* siRNA knockdown cells ( $n = 4$ ) compared to control siRNA-treated cells ( $n = 4$ ). (d) *MLLT11* siRNA knockdown leads to an increase in cells in the G1 phase and a decrease in cells in the S and G2 + M phases. (Left): Representative DNA profiles obtained from flow cytometry analysis of PI stained primary stromal cells 72 h after transfection with *MLLT11* siRNA or control siRNA. (Right): The percentage of cells in each cell cycle phase is plotted as mean + SD of primary stromal cells obtained from endometrial tissue of four different women without the disease. Data were analyzed using multiple *t*-test. (e) The p21 and p27 protein are significantly upregulated following *MLLT11* knockdown. Representative examples of Western blot analysis following *MLLT11* knockdown of p21 and p27, together with the GAPDH loading control. Densitometry of p21 and p27 protein levels from Western blots were normalized to the loading control. In (a–c,e), the results are expressed as scatter dot plots including the median relative expression levels in each group. Symbols—○: for control1, □: for control2, Δ: for control3, ◇: for control4. Data were analyzed using paired *t*-test (a–c) and Wilcoxon matched-pairs signed rank test (e). The *p* values < 0.05 were considered as significant.

Next, we addressed the consequences of this reduction in *MLLT11* levels on primary endometrial stroma cell biology. First, we assessed cell proliferation in these cells following *MLLT11* knockdown. We found that cell proliferation was significantly reduced by a median of 19.8% ( $p = 0.0002$ ) compared to the control knockdown cells (Figure 4c). Additionally, the knockdown of *MLLT11* in the control primary hESCs resembled the differences in the proliferation of the control and ectopic primary hESCs (EcESCs), showing reduced proliferation of EcESCs compared to the controls by a median of 13.6% ( $p = 0.031$ , Supplementary Figure S1b).

The knockdown of *MLLT11* was not associated with any change in cell survival, with no significant difference in apoptosis detected using a 7AAD/AnnexinV flow cytometry assay (Supplementary Figure S2a). A decrease in the *BCL2/BAX* ratio is another indication of apoptosis [24], and this did also not significantly differ between the *MLLT11* knockdown and control siRNA-transfected cells (Supplementary Figure S2b). However, *MLLT11* knockdown did affect the cell cycle, with a 7AAD flow cytometry assay showing a significant increase in the number of cells in the G1 phase (141.0%,  $\text{adjp} = 0.0003$ ) and a significant decrease in the number of cells in the S phase (73.9%,  $\text{adjp} = 0.053$ ) and G2/M phases (60.8%,  $\text{adjp} = 0.0006$ ) of the cell cycle (Figure 4d). This was associated with the significant upregulation of the levels of expression of the cell cycle checkpoint regulatory proteins p21 (1.39-fold,  $p = 0.033$ ) and p27 (3.11-fold,  $p$  value = 0.016) (Figure 4e). The increased levels of p27 protein under *MLLT11* knockdown was not associated with any significant changes in *CDKN1B* transcription (Supplementary Figure S1c). Therefore, *MLLT11* may act as negative post-transcriptional regulator of the gene in control hESCs. Overall, the G1 arrest observed in these experiments may explain the effect of *MLLT11* knockdown on proliferation.

### 2.3. *MLLT11* Mediates Camptothecin-Induced Apoptosis in Primary Endometrial Stroma Cells

It has been shown that *MLLT11* overexpression increases the sensitivity of human squamous cell carcinoma A431 parent (AP) cells and ovarian cancer cell lines to apoptotic drug stimulation [16,25]. Therefore, we tested whether reduced *MLLT11* expression in endometriosis lesions is associated with increased resistance to apoptotic stimuli. To do this, we added 1  $\mu\text{M}$  of the apoptosis-inducing agent camptothecin (CPT) to the medium 48 h after *MLLT11* or control knockdown and incubated for another 24 h before assessing the effect on apoptosis. Flow cytometry analysis of AnnexinV/7AAD positive cells to assess the number apoptotic cells showed no difference in the DMSO-treated cells (Figure 5a), consistent with an earlier experiment (Supplementary Figure S2a). However, while CPT treatment led to an increase in apoptotic cells in the control knockdown cells, apoptosis was not increased in the *MLLT11* knockdown cells, with 51.0% less apoptosis in *MLLT11* siRNA than in the control treated cells ( $\text{adjp} = 0.046$ ) (Figure 5a, right). This effect was associated with a significant increase in the *BCL2/BAX* ratio in the knockdown CPT-treated

cells (0.810 median fold change,  $\text{adj}p = 0.035$ ) compared to the control siRNA CPT-treated cells (Figure 5b left). These results indicate that *MLLT11* is involved in the regulation of CPT-induced apoptosis in primary endometrial stromal cells.

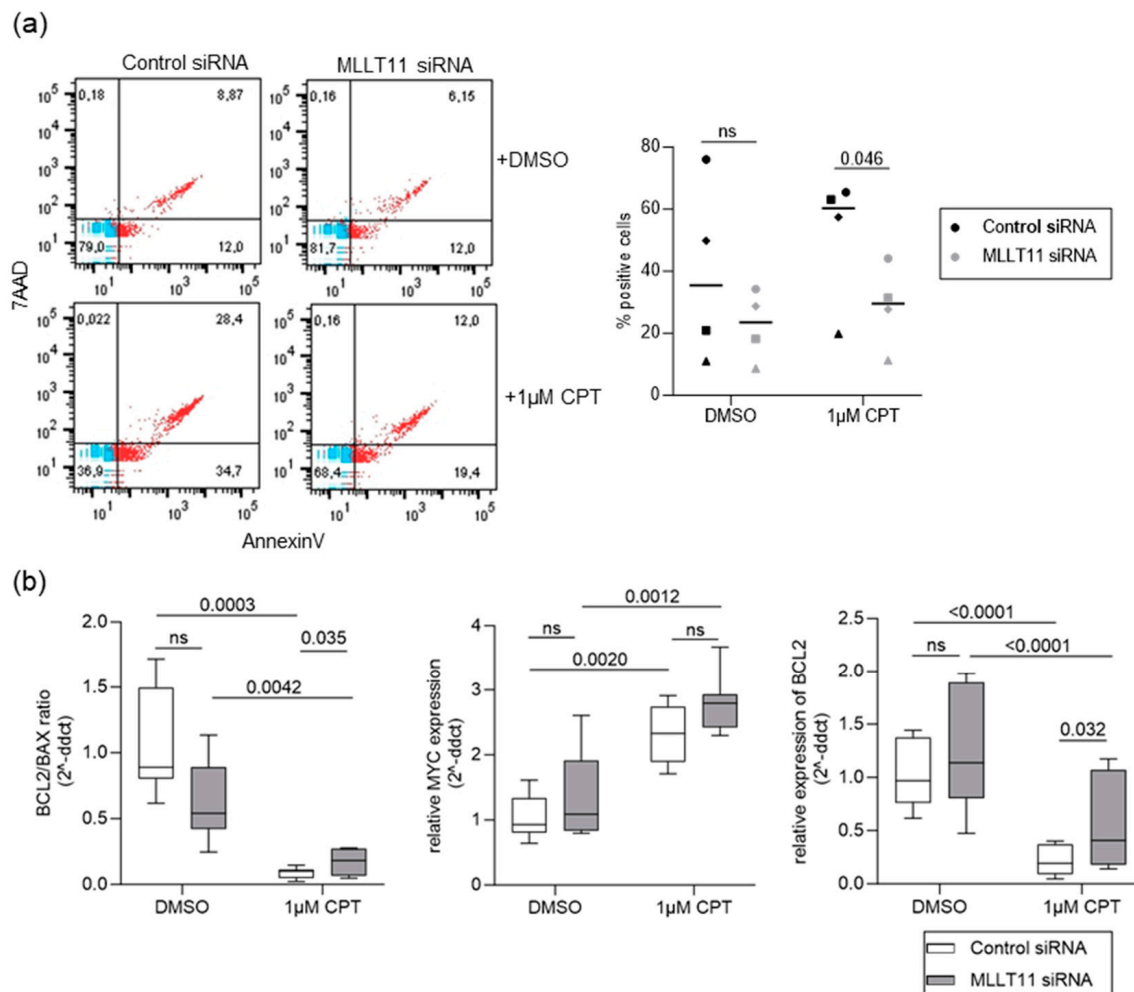


**Figure 5.** (a) Decreased number of apoptotic cells is seen in 24 h camptothecin (CPT)-treated cells 72 h after *MLLT11* siRNA knockdown. (Left): Representative flow cytometry scatter plots for AnnexinV+ versus 7-AAD+ cells. Primary stromal cells obtained from endometrial tissue of four women without endometriosis were treated for 24 h either with 0.1% DMSO or with 1  $\mu$ M CPT, together with either control siRNA or *MLLT11* siRNA for 72 h. (Right): No significant change in the number of apoptotic cells (AnnexinV+/7AAD (early apoptotic) plus AnnexinV+/7AAD+ (late apoptotic)) was observed between *MLLT11* knockdown and control siRNA-transfected cells in DMSO-treated cells. In CPT-treated cells, the number of total apoptotic cells was significantly decreased after *MLLT11* knockdown. The results are expressed as scatter dot plots including the median relative expression levels and interquartile ranges in each group. Symbols—○: for control1, □: for control2, Δ: for control3, ◇: for control4. Data were analyzed using paired *t*-test adjusted by Bonferroni correction, with *p* values < 0.05 considered as significant. (b) (Left), BCL2/BAX ratio (middle), relative cMYC expression (right), relative BCL2 expression in 24 h CPT-treated cells 72 h after *MLLT11* siRNA knockdown. Primary stromal cells obtained from eutopic endometrium of women without endometriosis were treated for 24 h either with 0.1% DMSO or with 1  $\mu$ M CPT, together with either control siRNA or *MLLT11* siRNA for 72 h. Results are expressed as box plots including Tukey whiskers. Data were analyzed using Sidak's multiple comparison tests from three biological replicates.

CTP-induced apoptosis in hESCs was associated with a significant upregulation in the levels of *c-MYC* expression (1.51 median fold change,  $\text{adj}p = 0.0020$  for control siRNA-treated cells and 1.57 median fold change,  $\text{adj}p = 0.0012$  for *MLLT11* siRNA-treated cells (Figure 5b, middle)), accompanied by downregulation of the level of *BCL2* expression (0.802 median fold change,  $\text{adj}p < 0.0001$  for control siRNA-treated cells and 0.643 median fold change,  $\text{adj}p < 0.0001$  for *MLLT11* siRNA-treated cells (Figure 5b right)) and a decreased *BCL2/BAX* ratio (0.887 median fold change,  $\text{adj}p = 0.0003$  for control siRNA-treated cells and 0.664 median fold change,  $\text{adj}p = 0.0042$  for *MLLT11* siRNA-treated cells (Figure 5b, left)) with or without *MLLT11* knockdown. However, *MLLT11* knockdown was associated with significant differences in the degree of *BCL2* transcriptional deregulation under CTP stimulation irrespective of the *c-MYC* levels. The *BCL2* expression was significantly lower in control siRNA-transfected cells compared to *MLLT11* knockdown cells (0.528 median fold change,  $\text{adj}p = 0.032$ ). Overall, these results indicate that *MLLT11* regulates the sensitivity of hESCs to CPT-induced apoptosis via the transcriptional regulation of *BCL2* expression.

#### 2.4. *MLLT11* Suppresses Adhesion in Primary Endometrial Stroma Cells of Women without Endometriosis

We evaluated the effect of *MLLT11* knockdown on stromal cell adhesion and invasion. The *MLLT11* knockdown did not significantly affect hESC invasion (Supplementary Figure S3a). Knockdown of *MLLT11* appeared to result in an increase in cellular adhesion at 10 min after plating on a collagen/fibronectin-coated plate (Figure 6a, left). Quantification confirmed that the number of adhered cells after 10 min was significantly increased in *MLLT11* knockdown cells (median change of 0.625,  $p = 0.001$ ) (Figure 6a, middle). Further, we measured the area covered by adhered cells. This also revealed a significant increase in the area covered by adherent cells following *MLLT11* knockdown (median change of 0.070,  $p = 0.002$ ) (Figure 6a, right). These data were consistent with the data obtained from the analysis of the differences in cellular adhesion in control and ectopic hESCs (Supplementary Figure S4). As for knockdown cells, the number of adhered cells in EcESM was increased (27.6% higher,  $p = 0.038$ ) when compared to hESC controls. The area of adhered cells in EcESM was 35.4% higher ( $p = 0.017$ ) compared to hESC controls (Supplementary Figure S4).

The adhesion of endometrial stroma cells is required to establish ectopic lesions. A positive association between the levels of expression of *MLLT11* and CD44, an adhesion molecule and direct target of the WNT/beta-catenin signaling, has been reported in breast cancer [17]. As reduced CD44 expression has been reported in the stroma cells of endometriosis lesions [26], we tested the effects of *MLLT11* knockdown on CD44 expression and WNT pathway activity. The results from the RT-qPCR analysis of CD44 (Supplementary Figure S3b) and Western blot analysis of active beta-catenin (Supplementary Figure S3c) in control siRNA and *MLLT11* siRNA-transfected hESCs show that these molecules are dispensable for the increase in adhesion seen in *MLLT11* knockdown cells.

Another gene associated with the regulation of cellular adhesion is *ACTA2* [27,28]. *ACTA2* is upregulated in ectopic lesions compared to eutopic controls in our cohort, irrespective of endometriosis disease severity (Figure 6b). Therefore, we analyzed the effect of *MLLT11* knockdown on *ACTA2* expression. We found that the *MLLT11* knockdown caused a significant increase in *ACTA2* at the mRNA (1.51 median fold increase;  $p = 0.008$ ) and protein level (1.46 median fold increase;  $p = 0.023$ ) compared to cells treated with control siRNA (Figure 6c). This effect was also associated with the upregulation of TGFB2 expression in *MLLT11* knockdown cells (1.63 median fold increase;  $p = 0.007$ ) compared to siRNA-treated control cells (Figure 6d).

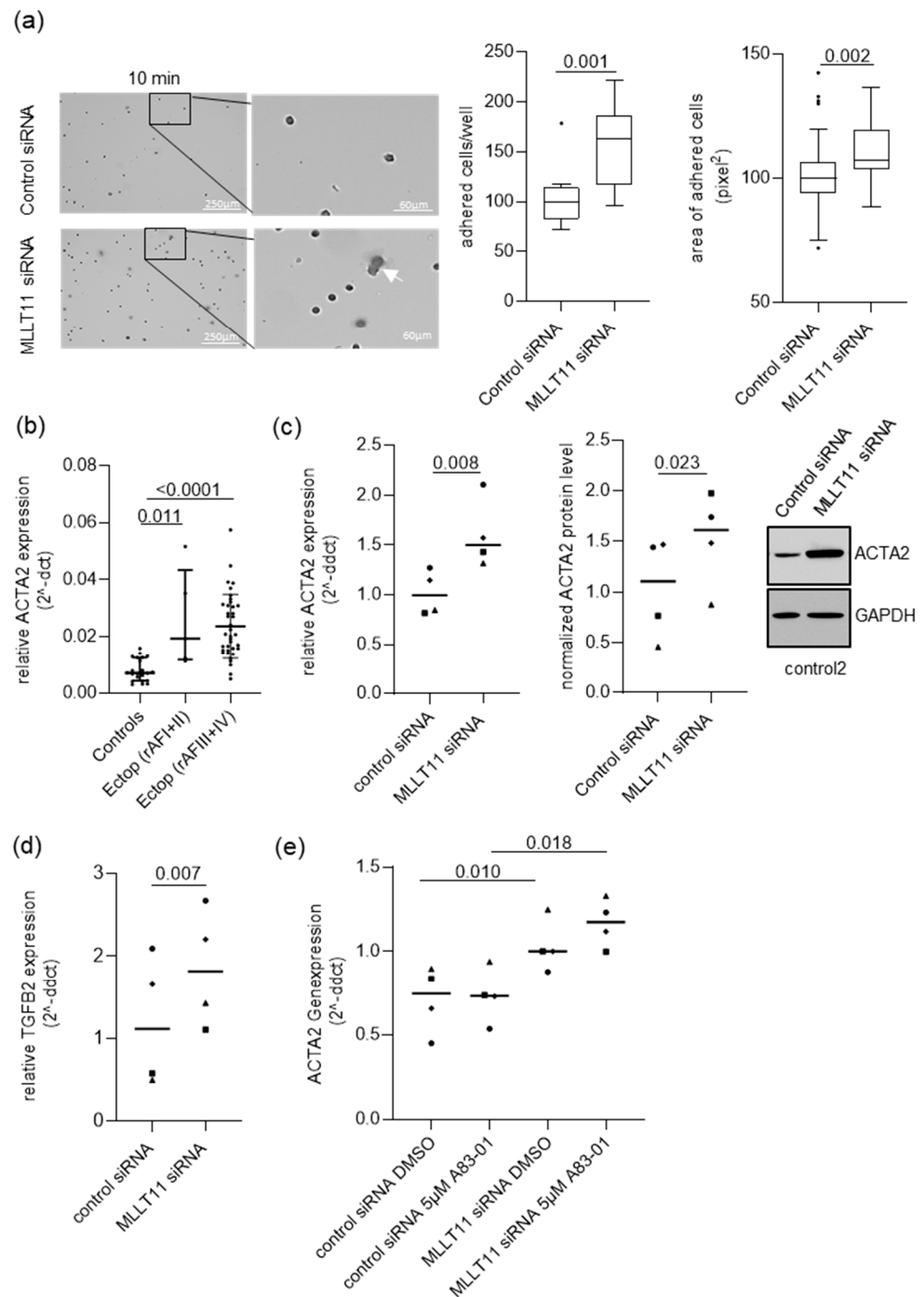


**Figure 6.** Number of adhering cells and area of adhesion are increased following *MLLT11* knockdown. **(a)** (Left): Representative images of control and knockdown cells at 100× and 400× magnification of the indicated magnified area stained with Chrystal Violet. The arrow shows a cell with increased adhesion area. (Middle): Quantification of the number of adhered cells to fibronectin- and collagen-coated plates after 72 h of *MLLT11* or control siRNA treatment stained 10 min after seeding. (Right): Quantification of the area of adhered cells to fibronectin- and collagen-coated plates after 72 h of *MLLT11* or control siRNA knockdown stained 10 min after seeding. Four independent image fields from three technical replicates in primary cells of four women were counted using ImageJ software V1.8.0. Results are expressed as boxplots with Tukey-based whiskers, and *p* values were calculated using the Wilcoxon matched-pairs signed rank test. **(b)** Gene expression of *ACTA2* is significantly increased in the ectopic lesions of women with mild (rAF I + II, n = 5) and high and more severe

(rAF III + IV, n = 38) endometriosis (revised American Fertility Society score) compared to the eutopic endometrium of women without endometriosis (n = 23). Gene expression of *ACTA2* was normalized to *ACTB* and data in (b) are presented as scatter dot plots including the median relative expression levels and interquartile ranges in each group. Data were analyzed using Mann–Whitney test adjusted using Bonferroni. (c) Altered gene expression and protein levels of *ACTA2* after *MLLT11* siRNA knockdown in primary stroma cells obtained from endometrial tissue of four women without the disease. Representative examples of Western blot analysis following *MLLT11* knockdown of *ACTA2*, together with the *GAPDH* loading control. Densitometric analysis of *ACTA2* levels from Western blots normalized to the loading control. (d) Altered gene expression levels of *TGFB2* after *MLLT11* siRNA knockdown in primary stroma cells obtained from endometrial tissue of four women without the disease. (e) The 24 h inhibition of the TGFB signaling by 5  $\mu$ M of A83-01 24 h after *MLLT11* siRNA knockdown in primary stroma cells obtained from endometrial tissue of four women without the disease. Gene expression of *ACTA2* and *TGFB2* in (c–e) were normalized to *GAPDH*, and results are expressed as scatter dot plots including the median relative expression levels in each group. Symbols—○: for control1, □: for control2, Δ: for control3, ◇: for control4. Data were analyzed using paired *t*-test, and *p* values < 0.05 were considered significant.

As *TGFB2* was previously reported to be a positive regulator of *ACTA2* expression [29,30], we tested if this is also true in *MLLT11* knockdown hESCs. We treated control siRNA and *MLLT11* siRNA-transfected cells with 5  $\mu$ M of A83-01 *TGFB2* inhibitor. Similar to untreated cells, as shown in Figure 6c, DMSO-treated cells showed an upregulation in *ACTA2* gene expression following *MLLT11* knockdown. However, this *ACTA2* upregulation was not reversed after *TGFB2* inhibition for 24 h (Figure 6e), indicating that, in endometrial stromal, the two genes are regulated independently by *MLLT11*.

### 3. Discussion

*MLLT11* is a gene implicated in hematopoietic progenitor cell differentiation [31] and neuronal cell differentiation [32]. In a pathogenic context, *MLLT11* has been reported to play an oncogenic role in the development and progression of a variety of human cancers [13–20] and to act as a tumor suppressor in glioma neural carcinomas [21]. However, the role for *MLLT11* in the pathogenesis of endometriosis has not been previously reported. In this study, we found that *MLLT11* protein is significantly downregulated in the endometriosis lesion stromal cells of women with Stage III and IV endometriosis. Given the small number of samples of women with Stage I + II endometriosis in our study, we cannot exclude that *MLLT11* is also downregulated in these patients. The knockdown of *MLLT11* in primary hESC of women without the disease leads to the downregulation of stromal cell proliferation, increased cell adhesion and reduced cell sensitivity to apoptotic stimuli. The effects of *MLLT11* knockdown on control hESC proliferation is due to disruption to the cell cycle, with G1 arrest and an impaired S phase associated with the upregulation of the cell cycle checkpoint proteins p21 and p27. Reduced proliferation endometriosis lesion stroma cells have been previously shown in vivo [9,33] and in vitro [34,35], and increased levels of p27 expression in endometriosis lesions have also been reported by several investigators [36,37]. Interestingly, Okamura et al. [36] showed that the levels of p27 increases with the progression of peritoneal endometriosis, with lower levels seen in highly vascularized and proliferating red peritoneal lesions compared to black lesions that show significantly lower proliferation based on the levels of Ki67 expression. Here, we show that reduced cell proliferation in *MLLT11* knockdown primary stromal cells from controls resembles the behavior of primary endometriosis stroma cells, which express significantly lower levels of *MLLT11* compared to controls. This indicates that *MLLT11* can act as a regulator of endometriosis lesion stroma cell proliferation in vivo and could be an important factor in disease progression. The mechanism by which *MLLT11* may regulate p21 and p27 protein expression in endometriosis remains unclear, but our data for p27 indicate that regulation occurs at a post-transcriptional level.

High levels of *MLLT11* were previously associated with low levels of p21 expression and increased proliferation in bladder cancer cells, where the levels of *MLLT11* have

been shown to be epigenetically regulated by miR-411 [19]. Mir-411 was identified as significantly upregulated in tissues of women with ovarian and peritoneal endometriosis compared to controls [38]. This indicates that a mechanism for the epigenetic regulation of *MLLT11* and *p21* expression, similar to those in bladder cancer, may exist in endometriosis. However, the discrete mechanisms of *MLLT11* and *MLLT11*-mediated *p21* regulation in endometriosis lesions remain to be experimentally tested.

In the context of hepatocellular, ovarian and squamous carcinoma and in promyelocytic leukemia cells, *MLLT11* was shown to exert proapoptotic functions [16,25,39]. However, the loss of *MLLT11* in developing cortical neurons had no impact on cell death [22]. In our cell system, CTP induces apoptosis through the transcriptional activation of *c-MYC*, leading to the downregulation of *BCL2* and the *BCL2/BAX* ratio. In general, the ability of *c-MYC* to induce apoptosis has been reported [40]. Previously, we could show a significant downregulation of *c-MYC* protein expression in the stromal compartment of ectopic endometriosis lesions, suggesting that cells with reduced *c-MYC* are more prone to survive apoptotic stimuli [41]. However, our data showed that *c-MYC* expression is not under the control of *MLLT11*. The knockdown of *MLLT11* in primary control hESCs did not affect the basal apoptosis levels or the *c-MYC* expression levels but showed a significant effect on the survival of CPT-treated cells. This was associated with changes in the degree of *BCL2* gene expression and the *BCL2*-to-*BAX* ratio in knockdown CPT-treated cells, leading to the enhanced antiapoptotic property of the cells.

CPT treatment can induce oxidative stress by enhancing the accumulation of intracellular reactive oxygen species (ROS) [42], leading to lipid peroxidation and lipid-derived electrophile accumulation [43], which induces cellular damage [44], normally leading to apoptosis. Oxidative stress is known as one of the main factors in endometriosis development and progression [45], and a decreased sensitivity of endometriosis lesion stroma cells to oxidative stress inducers has already been shown [46].

As CPT is a DNA topoisomerase 1 inhibitor, whose activity is higher in proliferating cells [43], the increased survival of control hESCs with reduced *MLLT11* expression to oxidative stress inducers, such as CTP, might be due to reduced proliferation and cell cycle arrest, accompanied by changes in the regulation of the *BAX* and *BCL2* signaling. Our data show that *MLLT11* might be an important factor in the regulation of cell survival in response to oxidative stress.

Furthermore, adhesion of endometrial tissue fragments to pelvic mesothelium is required for the formation of ectopic lesions. In our study, we demonstrated that *MLLT11* is a negative regulator of hESC adhesion. The increased adhesion following *MLLT11* knockdown in hESCs was accompanied by the significant transcriptional activation of *TGFB2* and *ACTA2* genes. Increased expression of *TGFB2* was found in ectopic lesions of women with endometriosis [47,48], and in rat models, high levels of *TGFB2* were associated with more advanced stages of the disease [47]. *TGFB2*, as positive regulator of *ACTA2* expression, was previously reported in bovine retinal pigment epithelial cells [30]. We have shown that inhibition of *TGFB2* signaling does not affect the expression of *ACTA2* in both control siRNA and *MLLT11* siRNA-transfected cells. Therefore, in endometriosis stroma cells, the *MLLT11* regulates *TGFB2* and *ACTA2* expression independently, and *TGFB2* signaling does not seem to be involved in the regulation of *ACTA2*. An increased level of *ACTA2* expression within ectopic endometriosis lesions compared to endometrium tissues from women without [49,50] and with endometriosis [37,49] was reported. In baboons, the intrastromal *ACTA2*-positive cells increased as the endometriotic lesions progressed [51], suggesting that *ACTA2* is associated with more advanced stages of the disease. We confirmed this observation and showed that *ACTA2* expression is more prominent in the endometriosis lesions of women with more advanced endometriosis.

We have shown that primary ectopic stroma cells of women with endometriosis, expressing lower levels of *MLLT11* and higher levels of *ACTA2*, compared to primary cells of women without the disease, displayed increased adhesive properties. Given that in vitro inhibition of *ACTA2* in myofibroblast cells leads to a significant decrease in adhesion due

to the reduction in the focal adhesion maturation [27], we speculate that the increased ACTA2 expression in *MLLT11* knockdown cells might increase the adhesive properties in these cells. Myofibroblasts are the main source of the extracellular matrix in fibrosis, and the myofibroblast differentiation of endometriosis stroma cells includes an activation of ACTA2 expression [52]. Therefore, the findings in the present study suggest that reduced *MLLT11* expression in endometriosis stroma cells may regulate the profibrotic capacity of these cells and contribute to endometriosis-associated fibrosis. However, additional experimental work needs to be performed to investigate the discrete mechanism of ACTA2 regulation and the role of ACTA2 in endometriosis stromal cell adhesion. A limitation of this study are the relative low numbers of patient samples, in particular from patients with mild endometriosis (rAF I + II), that were used.

Overall, our findings are consistent with a model in which a decreased expression of *MLLT11* promotes the persistence of endometriosis lesions outside of the uterus by increasing cell adhesion and enhancing the resistance of endometriosis stroma cells to oxidative-stress-mediated apoptosis. The low levels of expression of *MLLT11* in the stroma cells of endometriosis lesions are also consistent with the lack of uncontrolled proliferation of the lesions, ensuring the benign nature of the disease. However, whether the levels of *MLLT11* expression could correlate with transformation of the lesion from benign (low *MLLT11*) to a malignant (high *MLLT11*) phenotype, particularly in endometriosis-associated ovarian cancer, needs further investigation.

Our results indicate that *MLLT11* may be a new clinically relevant player in the pathogenesis of endometriosis, in particular in the advanced stages of the disease.

## 4. Materials and Methods

### 4.1. Study Population

Tissue was collected following the procedures of the Endometriosis Marker Austria (EMMA) study, a prospective study at the Tertiary Endometriosis Referral Center of the Medical University of Vienna. Premenopausal women aged 18–50 years that were given laparoscopic surgery due to suspected endometriosis, chronic pelvic pain, infertility, uterine leiomyoma or benign adnexal masses were invited to participate in the EMMA study. Ethics approval for this study was obtained from the Medical University of Vienna institutional ethics committee (EK 545/2010). Written and verbal informed consent from each patient was obtained before inclusion in the study. Detailed patient characteristics are summarized in Supplementary Table S1A–C. From the 70 women that participated in the study, 33 were endometriosis-free controls, and 37 were endometriosis patients. Endometriosis disease severity was defined by the revised American Fertility Society (rAFS) score. The control group were women subject to laparoscopic surgery due to uterine fibroids, fallopian tube disorders and benign ovarian cysts or due to unexplained chronic pelvic pain or infertility. Pregnant women and those breastfeeding within the last 6 months, as well as those who had received hormonal treatment within the last 3 months, were excluded from the study. Additionally excluded were women with known or suspected infectious disease, with acute inflammation and those with chronic autoimmune or malignant disease. Endometriosis was confirmed macroscopically by qualified surgeons and postsurgery through histological analysis by a pathologist. No endometriosis was detected in control patients at the time of the laparoscopic surgery. Control patients contributed one eutopic endometrium sample, while some endometriosis patients contributed multiple endometriosis lesion samples. All tissue samples were collected during diagnosis and/or therapy of endometriosis via curettage or laparoscopic surgical intervention. Samples were collected according to the Endometriosis Phenome and Biobanking Harmonization Project guidelines [53].

### 4.2. RNA Isolation

Frozen tissue samples taken from 31 control patients and 23 endometriosis patients were homogenized with a Precellys 24 homogenizer (Supplementary Table S1A, PEQLAB, Erlangen, Germany). Total RNA was then isolated from eutopic and ectopic endometrium

samples using the Agilent Absolutely Total RNA kit, which includes DNaseI treatment (Agilent, Santa Clara, CA, USA). Total RNA was isolated from primary stromal cells using the RNeasy mini kit (Qiagen, Venlo, The Netherlands) and then treated with DNaseI using the RapidOut DNA removal Kit (Thermo Fisher Scientific, Waltham, MA, USA). RNA concentration and purity were then measured using a NanoDrop ND-1000 spectrophotometer (NanoDrop Technologies, Wilmington, DE, USA). We defined the RNA quality as sufficient when the OD260/280 and OD260/230 ratios were around 2.00.

#### 4.3. Quantitative Reverse Transcription PCR (RT-qPCR)

RNA was reverse transcribed with the SuperScript<sup>®</sup> III First-Strand Synthesis Reverse Transcriptase kit using a mixture of oligo-d (T) and random hexamer primers (Life Sciences Advance Technology, St. Petersburg, FL, USA). We then diluted the cDNA 2-fold with water before assaying gene expression with quantitative reverse transcription PCR (RT-qPCR). Each RT-qPCR reaction contained 1× TaqMan master mix (Applied Biosystems, Waltham, MA, USA with ROX reference dye) and one of the gene expression TaqMan Assays listed in Supplementary Table S2A. RT-qPCR was conducted using a 7500 Fast Real-Time PCR System (Applied Biosystems, Waltham, MA, USA), with an initial denaturation step for 10 min at 95 °C, followed by 40 cycles of 15 s at 95 °C and 1 min at 60 °C. Relative expression of target genes was calculated using either the  $-\Delta\Delta CT$  method for *in vitro* analysis as described [54] or using the  $-\Delta CT$  method for patient data analysis as described [55], with normalization to GAPDH or ACTB expression, as indicated in the figure legends.

#### 4.4. Immunohistochemistry

MLLT11 protein expression and cellular localization was detected using immunohistochemical (IHC) analyses of archival formalin-fixed, paraffin-embedded tissue samples from control (n = 24) and endometriosis cases (n = 19) collected in the pathology department of the Medical University of Vienna between 2012 and 2015 (Supplementary Table S1B). IHC staining was performed on three-micrometer-thick tissue sections following heat antigen retrieval with 10 mM sodium citrate buffer (pH = 6) and blocking with H<sub>2</sub>O<sub>2</sub> on Ultra V Block (Thermo Scientific, Ultra Vision LP Kit, TL-060-HL, Waltham, MA, USA).

The CD10 antibody (mouse IgG, NCL-CD10-270, Novocastra, Wetzlar, Germany) and the MLLT11 antibody (rabbit IgG, ab109016, Abcam, Cambridge, GB) were applied with antibody diluent and background reducing components buffer (Dako, S3022, Glostrup, Denmark). Kidney was used as a positive control for MLLT11 and placenta for CD10. Mouse IgG1 (760-2014, Ventana, CA, USA) and rabbit IgG (sc-2027, Santa Cruz, CA, USA) were used as isotype negative controls. The IHC signals were detected using Ultra Vision LP Kit after incubating the enhancer for 10 min and the HRP polymer for 15 min (Thermo Scientific, Ultra Vision LP Kit, TL-060-HL, MA, USA) and then further incubation with DAB-Substrate (Dako, K346811, Glostrup, Denmark) according to the manufacturer's protocol. Slides were counterstained in hematoxylin before they were dehydrated and mounted. Scoring and immunohistochemical analysis was performed, as described previously [56] and as outlined in the figure legends.

#### 4.5. Primary Endometrial Stromal Cell (hESC) Cultures

Endometrial tissue obtained from control patients by curettage or from ectopic lesions from endometriosis patients by laparoscopic surgery was used to make primary endometrial stromal cells as previously described [57]. Briefly, the tissue was minced and incubated with collagenase (Sigma-Aldrich, St. Louis, MO, USA) at 37 °C for 10 min, filtered and then cultured further, as previously documented [58]. The cells were cultured on fibronectin–collagen–(Gibco, Grand Island, NY, USA) coated dishes in DMEM-F12 without phenol red (Gibco) supplemented with 10% fetal bovine serum (FBS) (Gibco), 2 mM L-glutamine (Gibco) and 1% antibiotics–antimycotic (Gibco) up until a maximum of passage 7 in a 37 °C CO<sub>2</sub>-humidified incubator. The purity of these stromal cells was evaluated using immunofluorescence analysis with antibodies against vimentin (stromal cell marker), CD10

(endometrial stromal cell marker) and by qPCR using PECAM1 (endothelial marker) and EPCAM (epithelial marker). This method produces 95–99% pure stromal cells.

#### 4.6. Immunofluorescence

Next,  $2 \times 10^4$  primary cells were plated on fibronectin/collagen (Roche, Mannheim, Germany) and allowed to adhere overnight. Briefly, the adhered cells were fixed in 4% paraformaldehyde, incubated in 50 mM ammoniumchloride, permeabilized and blocked in 0.3% Triton-X-100 and PBS with 5% normal goat serum (5425) before incubation with the primary antibodies: vimentin (rabbit IgG, sc5565; Santa Cruz Biotechnology, Santa Cruz, CA, USA) and CD10 (mouse IgG, NCL-CD10-270, Novocastra). Antirabbit Alexa Fluor 488-conjugated phalloidin (A1494754, Invitrogen, Waltham, MA, USA) and antimouse (A11017, Invitrogen) were used to visualize vimentin (rabbit) and CD10 (mouse) staining, respectively. DAPI was used for nuclear staining (10236, Roche Diagnostics, Indianapolis, IN, USA). Rabbit IgG (sc-2027, Santa Cruz) and mouse IgG1 (760-2014, Ventana) were used as isotype controls. Epifluorescence imaging was performed using an Olympus BX50 microscope equipped with soft imaging system-F-View camera and Cell'P imaging software V2.1 (Olympus Austria Ges.m.b.H, Vienna, Austria).

#### 4.7. *MLLT11* Knockdown

The primary hESCs were cultured in complete culture cell medium on coated 6-well culture plates (Nunc, Thermo Fisher Scientific, Waltham, MA, USA) at a concentration of  $8 \times 10^4$  cells/well until 50% confluency. The cells were then transfected with a *MLLT11* targeting siRNA oligo or a nontargeting control siRNA oligo (Cat. 4390846, Ambion, Austin, TX, USA) at a final concentration of 10 nM using Lipofectamine RNAiMAX transfection reagent (Invitrogen by Life Technology, Waltham, MA, USA). Western blot analyses and phenotypic analysis of *MLLT11* knockdown cells for changes in cellular proliferation and invasion/adhesion were conducted 72 h post-transfection. RT-qPCR to assess relative RNA expression levels was conducted 48 h post-transfection.

#### 4.8. Protein Isolation and Western Blot

Cells were lysed in a whole-cell lysis buffer containing 1% Triton-X 100, 10 mM Tris-HCl, pH7.4, 150 mM NaCl and 5 mM EDTA. Phosphatase and a protease inhibitor cocktail (phosStop, cOmplete mini, EDTA free, Thermo Fisher Scientific, Waltham, MA, USA) were added to the lysis buffer immediately prior to use. A standard Bradford assay was used to determine the protein concentration. An equal amount of protein from each sample was then immunoblotted and incubated with primary antibodies for the proteins of interest (Supplementary Table S2B) overnight at 4 °C. Secondary antibodies were diluted in a Tris pH 8.0, 0.1% Tween 20 buffer and incubated with the sample for 1 h at room temperature. Bound antibodies were then detected with the horseradish peroxidase chemiluminescent Clarity Western ECL substrate (Bio-Rad Laboratories Inc., Hercules, CA, USA) and visualized on a ChemiDoc Imaging System (Bio-Rad Laboratories Inc., Hercules, CA, USA). Protein expression levels on the blot were then quantified using ImageJ Software V1.8.0 accessed on 2 July 2023 (<http://rsbweb.nih.gov/ij>).

#### 4.9. Flow Cytometry

We used standard propidium iodide (PI) DNA staining flow cytometry protocol to detect changes in the cell cycle following *MLLT11* knockdown. Briefly, per assay, we harvested  $1 \times 10^6$  cells 72 h post-siRNA knockdown and fixed them in 70% precooled ethanol for 2 h on ice. Following a PBS wash, the cells were resuspended in 10  $\mu$ L PI staining solution containing 0.5 mL PI/RNase (550825 and 51-6621-1E, BD Pharmingen™, Heidelberg, Germany) and incubated at room temperature for 10 min. PI positive cells were then quantified using flow cytometry. The effect of *MLLT11* knockdown on apoptosis was assessed using flow cytometry, following staining with an FITC-conjugated AnnexinV antibody (antibody 640906, Annexin V Binding Buffer, (422201), BioLegend, San Diego,

CA, USA) and the vital dye 7-amino-actomycin D (00-6993-50, eBioscience, San Diego, CA, USA). A total of 10,000 events were recorded for each sample, with unstained cells being used as an assay control.

#### 4.10. Proliferation Assay

The proliferation rate 72 h after *MLLT11* knockdown in primary endometrial stromal cells derived from control patients and from ectopic lesions from endometriosis patients was analyzed using the CyQuant direct cell proliferation assay (Invitrogen, Waltham, MA, USA). Cells were trypsinized 48 h post-transfection with *MLLT11* and control siRNA oligos, and 15,000 cells/well were seeded on 96 flat-bottom cell culture plates (Thermo Fisher Scientific, Roskilde, Denmark). After 12 h, the cells were stained for 1 h with 100  $\mu$ L CyQuant reaction, and then, fluorescence was measured on a Clariostarplus microplate reader fitted with appropriate filters (BMG Labtech, Ortenberg, Germany). Following correction for background fluorescence with a cell-free sample, a standard curve was calculated and used to estimate cell number. Experiments were performed in triplicate, and the mean number of proliferating cells plotted relative to control siRNA-treated cells and set to 1.

#### 4.11. Matrigel Invasion Assay

Invasion of cells through a matrigel barrier was detected with a Boyden chamber assay 48 h post-siRNA knockdown. For each assay, 15,000 cells were resuspended in 100  $\mu$ L media and added to a Matrigel-coated filter (Matrigel growth factor reduced (354,230); Corning Incorporated, Corning, NY, USA, 1% matrigel solution in PBS, filter: 6.5 mm diameter, 8  $\mu$ m pores, Corning Incorporated, Corning, NY, USA). Cells were left to invade for 12 h toward the bottom of the well containing media with 10% FCS. Cells on the lower surface of the filter were fixed with 4% PFA and stained with DAPI and were photographed with 10 $\times$  objective using the EVOS2000 microscope. The mean number of invaded cells was calculated over four independent fields, and the results of triplicate experiments presented. Cell counting was conducted using ImageJ software V1.8.0 accessed on 2 July 2023 (<http://rsbweb.nih.gov/ij>).

#### 4.12. Adhesion Assay

The ability of cells to adhere on fibronectin- and collagen-coated 24-well plates was measured. After 72 h of siRNA knockdown, 30,000 cells per assay were resuspended in 500  $\mu$ L of growth media supplemented with 10% *v/v* FCS and antibiotics. The cells were allowed to attach for 10 min or for 30 min and then fixed with ice cold methanol and stained with Chrystal Violet. Photos were taken using a EVOS2000 microscope (Thermo Fisher Scientific, Waltham, MA, USA) with an  $\times 10$  objective. The number of adhering cells per experiment was calculated by averaging the number of attached cells over four independent fields, with the results of triplicate experiments presented. Adhesion areas were calculated using the average number of pixels for each cell in a photographic field over four independent fields per experiment and expressed as averages of triplicate experiments. ImageJ software V1.8.0 accessed on 2 July 2023 was used for counting the number and the area of adhering cells (pixels<sup>2</sup>) accessed on 2 July 2023 (<http://rsbweb.nih.gov/ij>).

#### 4.13. Statistics

All statistical tests were performed using Prism (GraphPad Prism 9.0 software, La Jolla, CA, USA). The exact statistical procedures for each analysis are described in the corresponding figure legends.

**Supplementary Materials:** The following supporting information can be downloaded at: <https://www.mdpi.com/article/10.3390/ijms25010439/s1>.

**Author Contributions:** Conceptualization, K.P. and I.Y.; Data curation, K.P., M.W.-S., B.W., Z.B.-H., L.S., A.P., R.W. and I.Y.; Formal analysis, K.P., M.W.-S., B.W., Z.B.-H. and I.Y.; Funding acquisition, H.H.; Investigation, K.P., H.H., L.S., A.P. and R.W.; Methodology, K.P. and I.Y.; Project administration, K.P.; Resources, R.W.; Software, K.P.; Validation, Q.J.H.; Visualization, K.P.; Writing—original draft, K.P., Q.J.H. and I.Y.; Writing—review and editing, K.P., H.H., Q.J.H., L.S., A.P. and R.W. All authors have read and agreed to the published version of the manuscript.

**Funding:** This research was partially funded by the Ingrid Flick Foundation (FA751C0801) awarded to H.H.

**Institutional Review Board Statement:** The study was conducted in accordance with the Declaration of Helsinki and approved by the ethics committee of the Medical University of Vienna (EK 545/2010).

**Informed Consent Statement:** Verbal and written informed consent was obtained from each participant prior to inclusion into the study.

**Data Availability Statement:** Data are contained within the article or Supplementary Materials.

**Acknowledgments:** The authors would like to thank all the participants and health professionals involved in the present study. We want to thank our technical assistant Isabella Haslinger for her diligent work and constant assistance.

**Conflicts of Interest:** The authors declare no conflicts of interest. The funder had no role in the design of the study; in the collection, analyses, or interpretation of data; in the writing of the manuscript; or in the decision to publish the results.

## References

1. Shafrir, A.L.; Farland, L.V.; Shah, D.K.; Harris, H.R.; Kvaskoff, M.; Zondervan, K.; Missmer, S.A. Risk for and consequences of endometriosis: A critical epidemiologic review. *Best. Pract. Res. Clin. Obstet. Gynaecol.* **2018**, *51*, 1–15. [[CrossRef](#)] [[PubMed](#)]
2. Zondervan, K.T.; Becker, C.M.; Missmer, S.A. Endometriosis. *N. Engl. J. Med.* **2020**, *382*, 1244–1256. [[CrossRef](#)] [[PubMed](#)]
3. Agarwal, S.K.; Chapron, C.; Giudice, L.C.; Laufer, M.R.; Leyland, N.; Missmer, S.A.; Singh, S.S.; Taylor, H.S. Clinical diagnosis of endometriosis: A call to action. *Am. J. Obstet. Gynecol.* **2019**, *220*, 354.e1–354.e12. [[CrossRef](#)] [[PubMed](#)]
4. Klemmt, P.A.B.; Starzinski-Powitz, A. Molecular and Cellular Pathogenesis of Endometriosis. *Curr. Womens Health Rev.* **2018**, *14*, 106–116. [[CrossRef](#)]
5. Van Gorp, T.; Amant, F.; Neven, P.; Vergote, I.; Moerman, P. Endometriosis and the development of malignant tumours of the pelvis. A review of literature. *Best. Pract. Res. Clin. Obstet. Gynaecol.* **2004**, *18*, 349–371. [[CrossRef](#)] [[PubMed](#)]
6. Flores, I.; Rivera, E.; Ruiz, L.A.; Santiago, O.I.; Vernon, M.W.; Appleyard, C.B. Molecular profiling of experimental endometriosis identified gene expression patterns in common with human disease. *Fertil. Steril.* **2007**, *87*, 1180–1199. [[CrossRef](#)]
7. Abramiuk, M.; Grywalska, E.; Malkowska, P.; Sierawska, O.; Hryniewicz, R.; Niedzwiedzka-Rystwej, P. The Role of the Immune System in the Development of Endometriosis. *Cells* **2022**, *11*, 2028. [[CrossRef](#)]
8. Sundqvist, J.; Andersson, K.L.; Scarselli, G.; Gemzell-Danielsson, K.; Lalitkumar, P.G. Expression of adhesion, attachment and invasion markers in eutopic and ectopic endometrium: A link to the aetiology of endometriosis. *Hum. Reprod.* **2012**, *27*, 2737–2746. [[CrossRef](#)]
9. Scotti, S.; Regidor, P.A.; Schindler, A.E.; Winterhager, E. Reduced proliferation and cell adhesion in endometriosis. *Mol. Hum. Reprod.* **2000**, *6*, 610–617. [[CrossRef](#)]
10. Bhyan, S.B.; Zhao, L.; Wee, Y.; Liu, Y.; Zhao, M. Genetic links between endometriosis and cancers in women. *PeerJ* **2019**, *7*, e8135. [[CrossRef](#)]
11. Saavalainen, L.; Lassus, H.; But, A.; Tiitinen, A.; Harkki, P.; Gissler, M.; Pukkala, E.; Heikinheimo, O. Risk of Gynecologic Cancer According to the Type of Endometriosis. *Obstet. Gynecol.* **2018**, *131*, 1095–1102. [[CrossRef](#)] [[PubMed](#)]
12. Banz, C.; Ungethuen, U.; Kuban, R.J.; Diedrich, K.; Lengyel, E.; Hornung, D. The molecular signature of endometriosis-associated endometrioid ovarian cancer differs significantly from endometriosis-independent endometrioid ovarian cancer. *Fertil. Steril.* **2010**, *94*, 1212–1217. [[CrossRef](#)] [[PubMed](#)]
13. Tiberio, P.; Lozneau, L.; Angeloni, V.; Cavadini, E.; Pinciroli, P.; Callari, M.; Carcangiu, M.L.; Lorusso, D.; Raspagliesi, F.; Pala, V.; et al. Involvement of AF1q/MLLT11 in the progression of ovarian cancer. *Oncotarget* **2017**, *8*, 23246–23264. [[CrossRef](#)] [[PubMed](#)]
14. Tse, W.; Zhu, W.; Chen, H.S.; Cohen, A. A novel gene, AF1q, fused to MLL in t(1;11) (q21;q23), is specifically expressed in leukemic and immature hematopoietic cells. *Blood* **1995**, *85*, 650–656. [[CrossRef](#)] [[PubMed](#)]
15. Strunk, C.J.; Platzbecker, U.; Thiede, C.; Schaich, M.; Illmer, T.; Kang, Z.; Leahy, P.; Li, C.; Xie, X.; Laughlin, M.J.; et al. Elevated AF1q expression is a poor prognostic marker for adult acute myeloid leukemia patients with normal cytogenetics. *Am. J. Hematol.* **2009**, *84*, 308–309. [[CrossRef](#)] [[PubMed](#)]
16. Tiberio, P.; Cavadini, E.; Callari, M.; Daidone, M.G.; Appierto, V. AF1q: A novel mediator of basal and 4-HPR-induced apoptosis in ovarian cancer cells. *PLoS ONE* **2012**, *7*, e39968. [[CrossRef](#)] [[PubMed](#)]

17. Park, J.; Schleder, M.; Schreiber, M.; Ice, R.; Merkel, O.; Bilban, M.; Hofbauer, S.; Kim, S.; Addison, J.; Zou, J.; et al. AF1q is a novel TCF7 co-factor which activates CD44 and promotes breast cancer metastasis. *Oncotarget* **2015**, *6*, 20697–20710. [[CrossRef](#)]
18. Liao, J.; Chen, H.; Qi, M.; Wang, J.; Wang, M. MLLT11-TRIL complex promotes the progression of endometrial cancer through PI3K/AKT/mTOR signaling pathway. *Cancer Biol. Ther.* **2022**, *23*, 211–224. [[CrossRef](#)]
19. Jin, H.; Sun, W.; Zhang, Y.; Yan, H.; Liufu, H.; Wang, S.; Chen, C.; Gu, J.; Hua, X.; Zhou, L.; et al. MicroRNA-411 Downregulation Enhances Tumor Growth by Upregulating MLLT11 Expression in Human Bladder Cancer. *Mol. Ther. Nucleic Acids* **2018**, *11*, 312–322. [[CrossRef](#)]
20. Kadletz, L.C.; Brkic, F.F.; Jank, B.J.; Schneider, S.; Cede, J.; Seemann, R.; Gruber, E.S.; Gurnhofer, E.; Heiduschka, G.; Kenner, L. AF1q Expression Associates with CD44 and STAT3 and Impairs Overall Survival in Adenoid Cystic Carcinoma of the Head and Neck. *Pathol. Oncol. Res.* **2020**, *26*, 1287–1292. [[CrossRef](#)]
21. Chen, L.; Xiong, Z.; Zhao, H.; Teng, C.; Liu, H.; Huang, Q.; Wanggou, S.; Li, X. Identification of the novel prognostic biomarker, MLLT11, reveals its relationship with immune checkpoint markers in glioma. *Front. Oncol.* **2022**, *12*, 889351. [[CrossRef](#)] [[PubMed](#)]
22. Stanton-Turcotte, D.; Hsu, K.; Moore, S.A.; Yamada, M.; Fawcett, J.P.; Iulianella, A. Mllt11 Regulates Migration and Neurite Outgrowth of Cortical Projection Neurons during Development. *J. Neurosci.* **2022**, *42*, 3931–3948. [[CrossRef](#)] [[PubMed](#)]
23. Toki, T.; Shimizu, M.; Takagi, Y.; Ashida, T.; Konishi, I. CD10 is a marker for normal and neoplastic endometrial stromal cells. *Int. J. Gynecol. Pathol.* **2002**, *21*, 41–47. [[CrossRef](#)] [[PubMed](#)]
24. Raisova, M.; Hossini, A.M.; Eberle, J.; Riebeling, C.; Wieder, T.; Sturm, I.; Daniel, P.T.; Orfanos, C.E.; Geilen, C.C. The Bax/Bcl-2 ratio determines the susceptibility of human melanoma cells to CD95/Fas-mediated apoptosis. *J. Invest. Dermatol.* **2001**, *117*, 333–340. [[CrossRef](#)] [[PubMed](#)]
25. Co, N.N.; Tsang, W.P.; Wong, T.W.; Cheung, H.H.; Tsang, T.Y.; Kong, S.K.; Kwok, T.T. Oncogene AF1q enhances doxorubicin-induced apoptosis through BAD-mediated mitochondrial apoptotic pathway. *Mol. Cancer Ther.* **2008**, *7*, 3160–3168. [[CrossRef](#)] [[PubMed](#)]
26. Poncelet, C.; Leblanc, M.; Walker-Combrouze, F.; Soriano, D.; Feldmann, G.; Madelenat, P.; Scoazec, J.Y.; Darai, E. Expression of cadherins and CD44 isoforms in human endometrium and peritoneal endometriosis. *Acta Obstet. Gynecol. Scand.* **2002**, *81*, 195–203. [[CrossRef](#)] [[PubMed](#)]
27. Hinz, B.; Dugina, V.; Ballestrem, C.; Wehrle-Haller, B.; Chaponnier, C. Alpha-smooth muscle actin is crucial for focal adhesion maturation in myofibroblasts. *Mol. Biol. Cell* **2003**, *14*, 2508–2519. [[CrossRef](#)]
28. Lee, H.W.; Park, Y.M.; Lee, S.J.; Cho, H.J.; Kim, D.H.; Lee, J.I.; Kang, M.S.; Seol, H.J.; Shim, Y.M.; Nam, D.H.; et al. Alpha-smooth muscle actin (ACTA2) is required for metastatic potential of human lung adenocarcinoma. *Clin. Cancer Res.* **2013**, *19*, 5879–5889. [[CrossRef](#)]
29. Mytilinaiou, M.; Bano, A.; Nikitovic, D.; Berdiaki, A.; Voudouri, K.; Kalogeraki, A.; Karamanos, N.K.; Tzanakakis, G.N. Syndecan-2 is a key regulator of transforming growth factor beta 2/Smad2-mediated adhesion in fibrosarcoma cells. *IUBMB Life* **2013**, *65*, 134–143. [[CrossRef](#)]
30. Kurosaka, D.; Muraki, Y.; Inoue, M.; Katsura, H. TGF-beta 2 increases alpha-smooth muscle actin expression in bovine retinal pigment epithelial cells. *Curr. Eye Res.* **1996**, *15*, 1144–1147. [[CrossRef](#)]
31. Parcelier, A.; Maharzi, N.; Delord, M.; Robledo-Sarmiento, M.; Nelson, E.; Belakhdar-Mekid, H.; Pla, M.; Kuranda, K.; Parietti, V.; Goodhardt, M.; et al. AF1q/MLLT11 regulates the emergence of human prothymocytes through cooperative interaction with the Notch signaling pathway. *Blood* **2011**, *118*, 1784–1796. [[CrossRef](#)] [[PubMed](#)]
32. Yamada, M.; Clark, J.; Iulianella, A. MLLT11/AF1q is differentially expressed in maturing neurons during development. *Gene Expr. Patterns* **2014**, *15*, 80–87. [[CrossRef](#)] [[PubMed](#)]
33. Beliard, A.; Noel, A.; Foidart, J.M. Reduction of apoptosis and proliferation in endometriosis. *Fertil. Steril.* **2004**, *82*, 80–85. [[CrossRef](#)] [[PubMed](#)]
34. Delbandi, A.A.; Mahmoudi, M.; Shervin, A.; Akbari, E.; Jeddi-Tehrani, M.; Sankian, M.; Kazemnejad, S.; Zarnani, A.H. Eutopic and ectopic stromal cells from patients with endometriosis exhibit differential invasive, adhesive, and proliferative behavior. *Fertil. Steril.* **2013**, *100*, 761–769. [[CrossRef](#)]
35. Yang, H.; Hu, T.; Hu, P.; Qi, C.; Qian, L. miR-143-3p inhibits endometriotic stromal cell proliferation and invasion by inactivating autophagy in endometriosis. *Mol. Med. Rep.* **2021**, *23*, 356. [[CrossRef](#)] [[PubMed](#)]
36. Matsuzaki, S.; Canis, M.; Murakami, T.; Dechelotte, P.; Bruhat, M.A.; Okamura, K. Expression of the cyclin-dependent kinase inhibitor p27Kip1 in eutopic endometrium and peritoneal endometriosis. *Fertil. Steril.* **2001**, *75*, 956–960. [[CrossRef](#)] [[PubMed](#)]
37. Meola, J.; Rosa e Silva, J.C.; Dentillo, D.B.; da Silva, W.A., Jr.; Veiga-Castelli, L.C.; Bernardes, L.A.; Ferriani, R.A.; de Paz, C.C.; Giuliatti, S.; Martelli, L. Differentially expressed genes in eutopic and ectopic endometrium of women with endometriosis. *Fertil. Steril.* **2010**, *93*, 1750–1773. [[CrossRef](#)] [[PubMed](#)]
38. Braza-Boils, A.; Mari-Alexandre, J.; Gilabert, J.; Sanchez-Izquierdo, D.; Espana, F.; Estelles, A.; Gilabert-Estelles, J. MicroRNA expression profile in endometriosis: Its relation to angiogenesis and fibrinolytic factors. *Hum. Reprod.* **2014**, *29*, 978–988. [[CrossRef](#)]
39. Co, N.N.; Tsang, W.P.; Tsang, T.Y.; Yeung, C.L.; Yau, P.L.; Kong, S.K.; Kwok, T.T. AF1q enhancement of gamma irradiation-induced apoptosis by up-regulation of BAD expression via NF-kappaB in human squamous carcinoma A431 cells. *Oncol. Rep.* **2010**, *24*, 547–554.
40. McMahon, S.B. MYC and the control of apoptosis. *Cold Spring Harb. Perspect. Med.* **2014**, *4*, a014407. [[CrossRef](#)]

41. Proestling, K.; Birner, P.; Gamperl, S.; Nirtl, N.; Marton, E.; Yerlikaya, G.; Wenzl, R.; Streubel, B.; Husslein, H. Enhanced epithelial to mesenchymal transition (EMT) and upregulated MYC in ectopic lesions contribute independently to endometriosis. *Reprod. Biol. Endocrinol.* **2015**, *13*, 75. [[CrossRef](#)] [[PubMed](#)]
42. Yokoyama, C.; Sueyoshi, Y.; Ema, M.; Mori, Y.; Takaishi, K.; Hisatomi, H. Induction of oxidative stress by anticancer drugs in the presence and absence of cells. *Oncol. Lett.* **2017**, *14*, 6066–6070. [[CrossRef](#)] [[PubMed](#)]
43. Flor, A.; Wolfgeher, D.; Li, J.; Hanakahi, L.A.; Kron, S.J. Lipid-derived electrophiles mediate the effects of chemotherapeutic topoisomerase I poisons. *Cell Chem. Biol.* **2021**, *28*, 776–787.e8. [[CrossRef](#)] [[PubMed](#)]
44. Cacciottola, L.; Donnez, J.; Dolmans, M.M. Can Endometriosis-Related Oxidative Stress Pave the Way for New Treatment Targets? *Int. J. Mol. Sci.* **2021**, *22*, 7138. [[CrossRef](#)] [[PubMed](#)]
45. Scutiero, G.; Iannone, P.; Bernardi, G.; Bonaccorsi, G.; Spadaro, S.; Volta, C.A.; Greco, P.; Nappi, L. Oxidative Stress and Endometriosis: A Systematic Review of the Literature. *Oxid. Med. Cell Longev.* **2017**, *2017*, 7265238. [[CrossRef](#)] [[PubMed](#)]
46. Malvezzi, H.; Cestari, B.A.; Meola, J.; Podgaec, S. Higher Oxidative Stress in Endometriotic Lesions Upregulates Senescence-Associated p16(ink4a) and beta-Galactosidase in Stromal Cells. *Int. J. Mol. Sci.* **2023**, *24*, 914. [[CrossRef](#)]
47. Sotnikova, N.Y.; Antsiferova, Y.S.; Posiseeva, L.V.; Shishkov, D.N.; Posiseev, D.V.; Filippova, E.S. Mechanisms regulating invasiveness and growth of endometriosis lesions in rat experimental model and in humans. *Fertil. Steril.* **2010**, *93*, 2701–2705. [[CrossRef](#)]
48. Yerlikaya, G.; Balendran, S.; Proestling, K.; Reischer, T.; Birner, P.; Wenzl, R.; Kuessel, L.; Streubel, B.; Husslein, H. Comprehensive study of angiogenic factors in women with endometriosis compared to women without endometriosis. *Eur. J. Obstet. Gynecol. Reprod. Biol.* **2016**, *204*, 88–98. [[CrossRef](#)]
49. Anaf, V.; Simon, P.; Fayt, I.; Noel, J. Smooth muscles are frequent components of endometriotic lesions. *Hum. Reprod.* **2000**, *15*, 767–771. [[CrossRef](#)]
50. Chen, M.; Zhou, Y.; Xu, H.; Hill, C.; Ewing, R.M.; He, D.; Zhang, X.; Wang, Y. Bioinformatic analysis reveals the importance of epithelial-mesenchymal transition in the development of endometriosis. *Sci. Rep.* **2020**, *10*, 8442. [[CrossRef](#)]
51. Zhang, Q.; Duan, J.; Olson, M.; Fazleabas, A.; Guo, S.W. Cellular Changes Consistent with Epithelial-Mesenchymal Transition and Fibroblast-to-Myofibroblast Transdifferentiation in the Progression of Experimental Endometriosis in Baboons. *Reprod. Sci.* **2016**, *23*, 1409–1421. [[CrossRef](#)] [[PubMed](#)]
52. Zhang, Z.; Wang, J.; Chen, Y.; Suo, L.; Chen, H.; Zhu, L.; Wan, G.; Han, X. Activin a promotes myofibroblast differentiation of endometrial mesenchymal stem cells via STAT3-dependent Smad/CTGF pathway. *Cell Commun. Signal* **2019**, *17*, 45. [[CrossRef](#)]
53. Fassbender, A.; Rahmioglu, N.; Vitonis, A.F.; Vigano, P.; Giudice, L.C.; D’Hooghe, T.M.; Hummelshoj, L.; Adamson, G.D.; Becker, C.M.; Missmer, S.A.; et al. World Endometriosis Research Foundation Endometriosis Phenome and Biobanking Harmonisation Project: IV. Tissue collection, processing, and storage in endometriosis research. *Fertil. Steril.* **2014**, *102*, 1244–1253. [[CrossRef](#)] [[PubMed](#)]
54. Livak, K.J.; Schmittgen, T.D. Analysis of relative gene expression data using real-time quantitative PCR and the 2<sup>(-Delta Delta C(T))</sup> Method. *Methods* **2001**, *25*, 402–408. [[CrossRef](#)] [[PubMed](#)]
55. Schmittgen, T.D.; Livak, K.J. Analyzing real-time PCR data by the comparative C(T) method. *Nat. Protoc.* **2008**, *3*, 1101–1108. [[CrossRef](#)]
56. Proestling, K.; Yotova, I.; Gamperl, S.; Hauser, C.; Wenzl, R.; Schneeberger, C.; Szabo, L.; Mairhofer, M.; Husslein, H.; Kuessel, L. Enhanced expression of TACE contributes to elevated levels of sVCAM-1 in endometriosis. *Mol. Hum. Reprod.* **2019**, *25*, 76–87. [[CrossRef](#)]
57. Tulac, S.; Overgaard, M.T.; Hamilton, A.E.; Jumbe, N.L.; Suchanek, E.; Giudice, L.C. Dickkopf-1, an inhibitor of Wnt signaling, is regulated by progesterone in human endometrial stromal cells. *J. Clin. Endocrinol. Metab.* **2006**, *91*, 1453–1461. [[CrossRef](#)]
58. Yotova, I.Y.; Quan, P.; Leditznig, N.; Beer, U.; Wenzl, R.; Tschugguel, W. Abnormal activation of Ras/Raf/MAPK and RhoA/ROCKII signalling pathways in eutopic endometrial stromal cells of patients with endometriosis. *Hum. Reprod.* **2011**, *26*, 885–897. [[CrossRef](#)]

**Disclaimer/Publisher’s Note:** The statements, opinions and data contained in all publications are solely those of the individual author(s) and contributor(s) and not of MDPI and/or the editor(s). MDPI and/or the editor(s) disclaim responsibility for any injury to people or property resulting from any ideas, methods, instructions or products referred to in the content.